

Title	Carrier localization and in-situ annealing effect on quaternary Ga _{1-x} In _x As _y Sb _{1-y} /GaAs quantum wells grown by Sb pre-deposition
Authors	Thoma, Jiri;Liang, Baolai;Lewis, Liam;Hegarty, Stephen P.;Huyet, Guillaume;Huffaker, Diana L.
Publication date	2013
Original Citation	Thoma, J., Liang, B., Lewis, L., Hegarty, S. P., Huyet, G. and Huffaker, D. L. (2013) 'Carrier localization and in-situ annealing effect on quaternary Ga _{1-x} In _x As _y Sb _{1-y} /GaAs quantum wells grown by Sb pre-deposition', Applied Physics Letters, 102(11), pp. 113101. doi: 10.1063/1.4795866
Type of publication	Article (peer-reviewed)
Link to publisher's version	http://aip.scitation.org/doi/abs/10.1063/1.4795866 - 10.1063/1.4795866
Rights	© 2013 American Institute of Physics.This article may be downloaded for personal use only. Any other use requires prior permission of the author and AIP Publishing. The following article appeared in Thoma, J., Liang, B., Lewis, L., Hegarty, S. P., Huyet, G. and Huffaker, D. L. (2013) 'Carrier localization and in-situ annealing effect on quaternary Ga _{1-x} In _x As _y Sb _{1-y} /GaAs quantum wells grown by Sb pre-deposition', Applied Physics Letters, 102(11), pp. 113101 and may be found at http://aip.scitation.org/doi/abs/10.1063/1.4795866
Download date	2023-05-07 20:45:17
Item downloaded from	http://hdl.handle.net/10468/4285



University College Cork, Ireland
Coláiste na hOllscoile Corcaigh

Carrier localization and in-situ annealing effect on quaternary $\text{Ga}_{1-x}\text{In}_x\text{As}_y\text{Sb}_{1-y}/\text{GaAs}$ quantum wells grown by Sb pre-deposition

Jiri Thoma, Baolai Liang, Liam Lewis, Stephen P. Hegarty, Guillaume Huyet, and Diana L. Huffaker

Citation: *Appl. Phys. Lett.* **102**, 113101 (2013); doi: 10.1063/1.4795866

View online: <http://dx.doi.org/10.1063/1.4795866>

View Table of Contents: <http://aip.scitation.org/toc/apl/102/11>

Published by the [American Institute of Physics](#)



Carrier localization and *in-situ* annealing effect on quaternary $\text{Ga}_{1-x}\text{In}_x\text{As}_y\text{Sb}_{1-y}/\text{GaAs}$ quantum wells grown by Sb pre-deposition

Jiri Thoma,^{1,2} Baolai Liang,³ Liam Lewis,¹ Stephen P. Hegarty,² Guillaume Huyet,^{1,2} and Diana L. Huffaker³

¹Centre for Advanced Photonics & Process Analysis, Cork Institute of Technology, Ireland

²Tyndall National Institute, UCC, Lee Maltings, Cork, Ireland

³Department of Electrical Engineering, California NanoSystems Institute, UCLA, Los Angeles, California 90095, USA

(Received 19 November 2012; accepted 7 March 2013; published online 18 March 2013)

Using temperature-dependent photoluminescence spectroscopy, we have investigated and compared intrinsic InGaAs, intrinsic GaInAsSb, and p-i-n junction GaInAsSb quantum wells (QWs) embedded in GaAs barriers. Strong carrier localization inside the intrinsic GaInAsSb/GaAs QW has been observed together with its decrease inside the p-i-n sample. This is attributed to the effect of an *in-situ* annealing during the top p-doped AlGaAs layer growth at an elevated temperature of 580 °C, leading to Sb-atom diffusion and even atomic redistribution. High-resolution X-ray diffraction measurements and the decrease of both maximum localization energy and full delocalization temperature in the p-i-n QW sample further corroborated this conclusion.

© 2013 American Institute of Physics. [<http://dx.doi.org/10.1063/1.4795866>]

GaAs-based semiconductor alloys are attracting attention for high-speed applications in many optoelectronic devices as a replacement for InP-based materials.^{1,2} Telecommunication networks are of particular interest, in which GaAs materials offer a mature technology,^{3,4} better integration with other optical elements,^{5,6} and better thermal properties.⁷ Most notably, InGaAs/GaAs quantum wells (QWs) have received significant attention in order to achieve emission at 1.31 μm and 1.55 μm . The lattice mismatch however limits the maximum In content and thus the longest achievable wavelength with reasonable epitaxial quality in two-dimensional (2D) growth mode. The highest emission wavelength reported for an InGaAs QW laser was at 1.24 μm for a highly strained material.^{8,9} Recently, much effort has been focused on exploring GaInAsN/GaAs QWs, where adding small amounts of nitrogen leads to favourable changes in band alignment and pushes the emission wavelength towards 1.31 μm .^{10–12} Unfortunately, N incorporation leads to a deterioration of the optical properties as defect induced nonradiative recombination (NRR) increases in line with increasing N concentration.¹³ This is largely detrimental for the gain properties, and although several methods^{14,15} have been proposed to increase the nitrogen concentration without worsening the material quality, the lowest lasing threshold current density reported (211 A/cm²) remains high.¹⁶ This has motivated the exploration of the effect of low temperature growth, combined with a Sb surfactant, allowing an increase of In concentration in 2D growth without reaching the critical thickness.¹⁷ In addition, the incorporation of Sb in InGaAs leads to a bandgap reduction that is favourable for the extension of the emission wavelength,¹⁸ while the optical quality increases, improving the device performance. The reported threshold current density of double QW lasers was as low as 125 A/cm² per well.¹⁹ These properties make a GaInSbAs material advantageous over GaInNAs.

Although reports on the quality of intrinsic GaInAsSb/GaAs QWs¹⁷ and the carrier localization effect²⁰ exist, the influence of *in-situ* annealing on the optical properties of the

QW during p-doped AlGaAs cladding layers growth remains unknown. Further, even though the reported photoluminescence (PL) emission wavelength was as long as 1250 nm,¹⁷ there is no explanation why the longest lasing wavelength achieved so far is 1167 nm.¹⁹

To shed some light on the influence of *in-situ* annealing, we have grown and studied three samples: the reference InGaAs QW; an intrinsic GaInAsSb QW; and a p-i-n GaInAsSb QW. The samples were grown on (100) GaAs substrates using a VEECO GEN-930 molecular beam epitaxy system. All samples were designed with 6 nm thickness of QW embedded in 100 nm GaAs barriers. The p-i-n sample intrinsic region (with thickness $w = 206$ nm, consisting of a 6 nm GaInAsSb QW within undoped 100 nm GaAs layers) was delimited by an upper p-doped and bottom n-doped $\text{Al}_{0.3}\text{Ga}_{0.7}\text{As}$ claddings (Table I). The QWs were grown at a temperature of 425 °C while the AlGaAs cladding layers were grown at a substrate temperature of 580 °C. The In and Ga growth rates were set at 0.15 ML/s and 0.35 ML/s, respectively, to keep the In/Ga ratio comparable for all three samples. The group V flux was set at beam equivalent pressure (BEP) of 2.0×10^{-6} Torr for As_2 and 4.0×10^{-7} Torr for Sb_2 , respectively. For all the samples, we confirm the 2-dimensional growth mode by RHEED during the QW growth. To improve the QW quality and allow proper incorporation of the big Sb atoms into InGaAs matrix, both the intrinsic and p-i-n samples were grown using the Sb pre-deposition method, in which a 25 s Sb-soak was conducted on GaAs surface before the QW growth.²⁰

We show in Fig. 1 the PL spectra for all three QW samples, taken at 14 K and room temperature (RT) of 293 K. The PL peak of the intrinsic QW sample at RT (0.988 eV) was shifted by 180 meV from the reference sample peak (1.167 eV). This difference was significantly lower for the p-i-n QW sample (1.066 eV), in which the PL peak shifted by 100 meV from the reference sample peak. Also notably, the redshift between 14 K and RT of the PL peak energies was

TABLE I. p-i-n sample structure with target dimensions and doping description.

Material	Thickness [nm]	Doping [cm^{-3}]
GaAs	100	1×10^{19}
p- $\text{Al}_{0.3}\text{GaAs}$	100	1×10^{18}
p- $\text{Al}_{0.3}\text{GaAs}$	50	5×10^{17}
GaAs	100	
$\text{Ga}_{0.70}\text{In}_{0.30}\text{As}_{0.875}\text{Sb}_{0.125}$	6	
GaAs	100	
n- $\text{Al}_{0.3}\text{GaAs}$	50	5×10^{17}
n- $\text{Al}_{0.3}\text{GaAs}$	100	1×10^{18}
GaAs buffer	100	1×10^{18}
n+ GaAs substrate		

lower for the Sb-containing samples than for the reference InGaAs sample (Table II). The improvement of optical quality with Sb addition was apparent from the PL linewidth measurement, the FWHM was lower by 6 meV for the intrinsic sample and 34 meV for the p-i-n sample with simultaneous achievement of emission at longer wavelengths at RT. The FWHM at 14 K behaved differently however; the intrinsic sample was 12 meV wider than the reference sample, while the p-i-n sample was 9 meV narrower (Table II). At this point, we must emphasize that the 100 meV peak shift of the p-i-n sample comprises a mixture of two counterbalancing parts; first one (large blueshift) induced by *in-situ* annealing; and second one (minimal redshift) induced by embedding the QW into p-i-n junction leading to the quantum-confined Stark effect. In our previous report,²¹ we studied an effect of applied electric field across the p-i-n sample and under the built-in electric field of 54 kV/cm the observed (almost negligible) redshift was about 2.2 meV (2.4 nm).

To clarify these points, we first studied the material composition by high-resolution $\langle 004 \rangle$ X-ray diffraction (HRXRD) analyses (Fig. 2) using a Bede D1 high resolution x-ray diffraction system. The observed PL emission peak relative positions (Fig. 1 solid blue and red) are explained by a decrease of Sb content from 13% (intrinsic sample) to 7% (p-i-n sample) evidenced by a rocking curve peak shifted from -7500 arcsec (Fig. 2 red), typical of an intrinsic sample,¹⁷ down to -6000 arcsec (Fig. 2 black). This might be a result of a strong atomic redistribution and decomposition during the AlGaAs layer growth at increased temperature due to large miscibility gap in GaInAsSb alloy.²² In this process, the big Sb-atoms diffuse out of the QW to the neighbouring GaAs barrier, thus resulting both in lower Sb content. To further corroborate the hypothesis of Sb-atoms (rather than atoms of In) reorganization, a sample containing 6 nm InGaAs QW and embedded into a full laser structure with AlGaAs claddings of 1500 nm thicknesses was grown

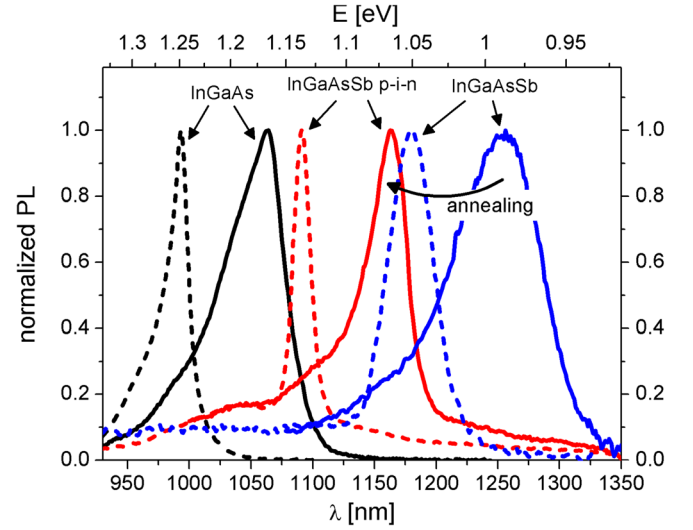


FIG. 1. PL spectra measured at RT (solid lines) and 14 K (dashed lines) for the reference InGaAs (black), intrinsic InGaAsSb (blue), and p-i-n InGaAsSb (red) QW samples.

simultaneously with the three samples presented. The RT PL peak was observed at 1.188 eV, i.e., only 20 meV shifted from the reference sample even though the cladding growth time at increased temperature was significantly ($10\times$) longer than for the p-i-n Sb QW.

Second, we have performed a set of temperature dependent PL to provide further insight into the quality of the QWs interfaces and effect of *in-situ* annealing during the top AlGaAs layers growth. Any inhomogeneity in thickness or composition manifests itself as an abnormal S-shaped temperature dependence of the PL peak position. This peculiarity, well-known for the quaternary GaInAsN/GaAs material,^{23–25} originates from the exciton localization effect inside the Sb-rich, quantum dot-like, regions of the quaternary GaInAsSb alloy.²⁰ The PL measurements were carried out as a function of temperature (14 K–290 K) at different, i.e., high (150 W/cm^2) and low (5 W/cm^2), excitation intensities (Fig. 3). At low excitation intensity, the S-shaped behavior characteristic of a localization effect at low temperature was clearly visible both for the intrinsic (blue) and the p-i-n sample (red), but this S-shape behavior was not longer visible for the reference InGaAs sample (black). At high excitation intensity, any potential localized states were saturated, resulting in a classical (monotonic) energy variation over the full temperature range and the PL peak energies following the Varshni model²⁶ (all the parameters $E(0)$, α , and β are given in Table III for all samples):

$$E(T) = E(0) - \frac{\alpha T^2}{T + \beta}. \quad (1)$$

TABLE II. Characteristics of the samples: The In-content x_{In} and the Sb-content y_{Sb} are determined by x-ray diffraction. The $E(\text{RT})$ and $E(14 \text{ K})$ stand for RT and 14 K PL energies; ΔE denotes the redshift between 14 K and RT; and FWHM stands for the PL linewidth.

Sample	x_{In} (%)	y_{Sb} (%)	$E(\text{RT})$ (eV)	$E(14 \text{ K})$ (eV)	ΔE (meV)	$\text{FWHM}(\text{RT})$ (meV)	$\text{FWHM}(14 \text{ K})$ (meV)
InGaAs	28	0	1.166	1.248	82	67.1	27.9
InGaAsSb	31	13	0.988	1.051	62	61.2	40.2
InGaAsSb pin	31	7	1.066	1.136	70	33.6	18.5

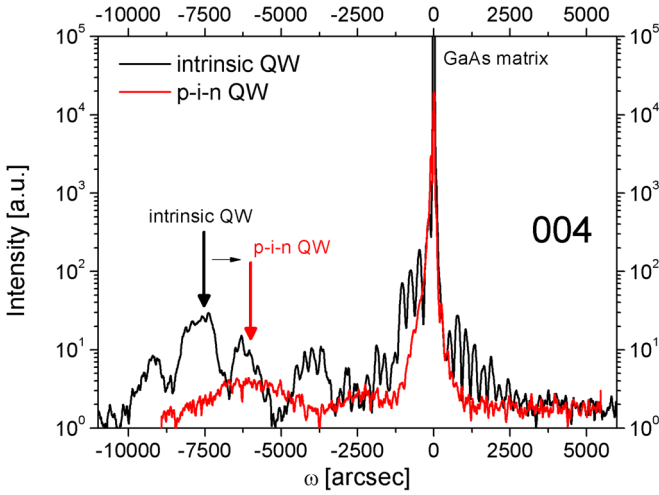


FIG. 2. Measured (004) X-ray rocking curves of the intrinsic (black) and p-i-n (red) samples, both grown with MBE using the Sb pre-deposition method under same conditions.

By examining both the excitation intensity variation and the energy difference $E_{loc}(T) = E(T) - E_{PL}(T)$ (where $E(T)$ is the middle-to-high temperature range fit using the Varshni model and $E_{PL}(T)$ is the PL peak energy at low excitation powers²⁵), we extract the carrier localization energies. The 14 K and the maximum localization energies are reported (Table III), together with the full delocalization temperatures. As mentioned above, the evolution of the PL peak energy for the InGaAs QW followed regular carrier thermalization with maximum localization energy of 2–3 meV and a delocalization temperature of 30 K. In the case of the GaInAsSb QW, the 14 K localization energy and the maximum localization energy were found to be 20 meV and 28 meV (intrinsic sample), and 13 meV and 17 meV (p-i-n sample), respectively (Fig. 4). Also the full delocalization temperatures have increased from 30 K to 170 K and 100 K.

This decrease in carrier localization energy inside the p-i-n sample is another consequence of the atomic reorganization. The *in-situ* annealing leads to a more even atomic distribution, alleviating the presence of Sb-rich clusters on

TABLE III. The Varshni model parameters $E(0)$, α , β ; $E_{loc}(14\text{ K})$ denotes the localization energy at 14 K; E_{loc}^{max} is the maximum localization energy, and T_{deloc} stands for the full delocalization energy.

Sample	$E(0)$ (eV)	$\alpha(10^{-4})$ (eV K ⁻¹)	β (K)	$E_{loc}(14\text{ K})$ (meV)	E_{loc}^{max} (meV)	T_{deloc} (K)
InGaAs	1.25	6.545	345	2–3	2–3	30
InGaAsSb	1.05	8.11	751	20	28	170
InGaAsSb pin	1.137	8	609	13	17	100

the QW interface and thus lowering the exciton localization energy.

Finally, to confirm an improved QW quality and smoother interface of the p-i-n QW over the intrinsic QW, both samples were observed by transmission electron microscope (TEM). The cross-sectional TEM images (Fig. 5) show no mismatch dislocations for both samples, but obvious interface roughness and faceting is visible at the top interface for the intrinsic sample (Fig. 5(a)). The sharpness and homogeneity of the p-i-n sample interface (Fig. 5(b)) further supports the above hypotheses.

In summary, the impact of top AlGaAs layer growth at elevated temperature of full p-i-n junction on GaInAsSb/GaAs QW has been investigated. Two features have been observed: first, the blueshift of PL emission from 1254 nm (intrinsic sample) to 1163 nm (p-i-n sample) together with the shift of the QW rocking curves peaks in the XRD analysis is explained by decrease of Sb composition from 13% to 7% inside the QW; second, the decrease of carrier localization energy accompanied by decrease of full delocalization temperature in the p-i-n sample is explained by more evenly distributed atoms on the QW interface alleviating any changes in composition and thus possible In-rich and Sb-rich regions. Both features are impacts of Sb-atom redistribution and Sb diffusion out to the surrounding GaAs barrier. One method to mitigate the undesired blueshift of the QW emission is to cap (overgrow) the actual GaInAsSb QW by a very thin GaAsSb layer with several beneficial impacts.²⁷ First, it would reduce any Sb diffusion out of the QW into

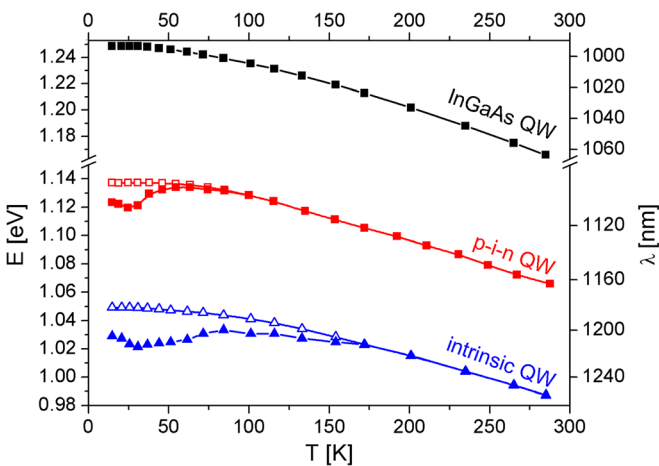


FIG. 3. Evolution of the PL peak energy for all three QWs in the temperature of 14 K–290 K under low (full) and high (open) excitation power intensities for reference InGaAs (black), intrinsic InGaAsSb (blue), and p-i-n InGaAsSb (red) QW samples.

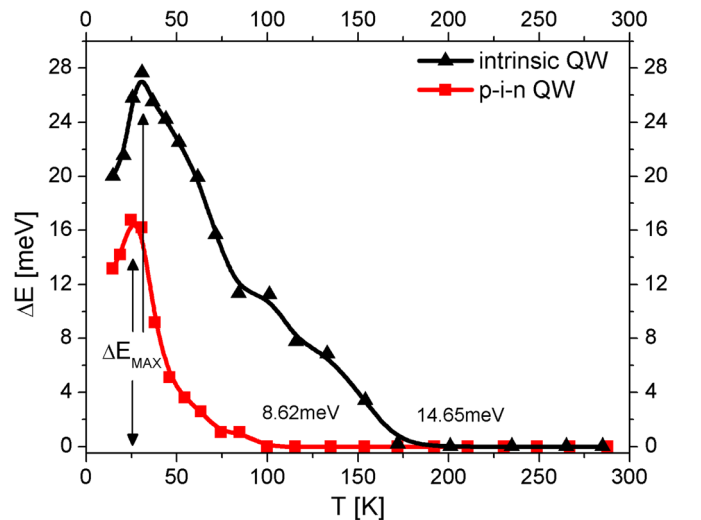


FIG. 4. Temperature dependent carrier localization energies for the intrinsic sample (black) and the p-i-n sample (red).

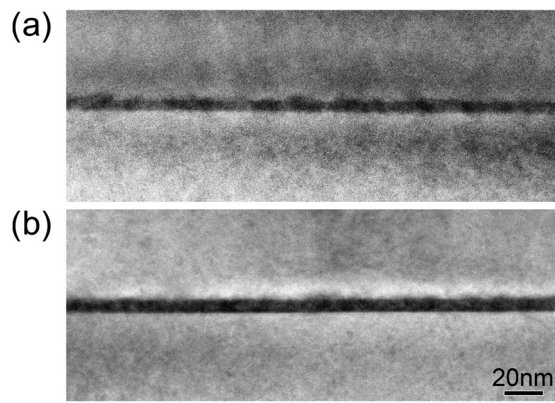


FIG. 5. A cross-sectional TEM image of the (a) intrinsic QW sample and (b) p-i-n QW sample showing better QW quality.

surrounding barrier during the top cladding layer growth at elevated temperature, and thus it would reduce the undesired PL peak blueshift. Second, using this capping layer would substantially lower the abrupt step of lattice mismatch between the quaternary and binary alloys, mitigating any fluctuation of QW thickness or composition and thus decreasing QWs FWHM. Finally, reducing this lattice mismatch would also mitigate a presence of defects leading to decreasing device efficiency on behalf of nonradiative recombination. Next possible method to improve QW FWHM and to simultaneously reduce significant QW blueshift lies in embedding the quaternary structure inside thin graded InGaAs layers.²⁸ This scheme would lower lattice mismatch between the binary GaAs barriers and the quaternary GaInAsSb QW and could lead to similar effects as described above. Another suggesting idea lies in combining the two above in form of graded GaAsSb layer. To reduce this blueshift or even push the GaInAsSb QW emission toward 1310 nm could be possible taking into account combination of several approaches or even separately. First one lies in using of capping layers already mentioned reducing any Sb leakage. Second, we would reduce an impact of *in-situ* annealing by lowering the growth temperature of the top cladding layers down to 520 °C, but this could also affect the cladding layers quality and thus lasing properties. Finally, further redshift of QW emission could be achieved simply by growing a QW with higher thickness thus lowering the bandgap energy. This would also lead to an increase of device modal gain by increasing confinement factor Γ , but one must be careful not to achieve the critical thickness of the 2D growth mode.

This work was supported by the Science Foundation Ireland (SFI) Strategic Research Cluster, PiFAS, under Contract No. 07/SRC/I1173. The authors also gratefully acknowledge the financial support of United States Department of Defense (Grant NSSEFF N00244-09-1-0091).

- ¹G. P. Agrawal, *Fiber-Optic Communication Systems* (Wiley Series Hardcover, (2010).
- ²M. S. Alias, S. M. Mitani, and F. Maskurty, *Optik* **123**, 1051 (2011).
- ³J. S. Harris, *Semicond. Sci. Technol.* **17**, 880 (2002).
- ⁴G. Adolfsson, S. Wang, M. Sadeghi, J. Bengtsson, A. Larsson, J. J. Lim, V. Vilokinen, and P. Melanen, *IEEE J. Quantum Electron.* **44**, 607 (2008).
- ⁵M. Kondow, T. Kitatani, S. Nakatsuka, M. C. Larson, K. Nakahara, Y. Yazawa, M. Okai, and K. Uomi, *IEEE J. Sel. Top. Quantum Electron.* **3**, 719 (1997).
- ⁶A. Yu. Egorov, A. E. Zhukov, and V. M. Ustinov, *J. Electron. Mater.* **30**, 477 (2001).
- ⁷M. Kondow, K. Uomi, A. Niwa, T. Kitatani, S. Watahiki, and Y. Yazawa, *Jpn. J. Appl. Phys., Part 1* **35**, 1273 (1996).
- ⁸P. Sundgren, J. Berggren, P. Goldman, and M. Hammar, *Appl. Phys. Lett.* **87**, 071104 (2005).
- ⁹L. W. Sun and H. H. Lin, *Appl. Phys. Lett.* **83**, 1107 (2003).
- ¹⁰N. Tansu and L. J. Mawst, *Appl. Phys. Lett.* **82**, 1500 (2003).
- ¹¹N. Tansu, J.-Y. Yeh, and L. J. Mawst, *Appl. Phys. Lett.* **83**, 2512 (2003).
- ¹²S. Wu and L. Wan, *J. Appl. Phys.* **110**, 123109 (2011).
- ¹³R. Fehse, S. Tomic, A. R. Adams, S. J. Sweeney, E. P. O'Reilly, A. Andreev, and H. Riechert, *IEEE J. Sel. Top. Quantum Electron.* **8**, 801 (2002).
- ¹⁴N. Tansu, J. Yeh, and L. J. Mawst, *J. Phys.: Condens. Matter* **16**, S3277 (2004).
- ¹⁵A. Albo, G. Bahir, and D. Fekete, *J. Appl. Phys.* **108**, 093116 (2010).
- ¹⁶N. Tansu, N. J. Kirsch, and L. J. Mawst, *Appl. Phys. Lett.* **81**, 2523 (2002).
- ¹⁷D. Jiang, Y.-H. Qu, H.-Q. Ni, D.-H. Wu, Y.-Q. Xu, and Z.-Ch. Niu, *J. Cryst. Growth* **288**, 12 (2006).
- ¹⁸J. C. Harmand, L. H. Li, G. Patriarche, and L. Travers, *Appl. Phys. Lett.* **84**, 3981 (2004).
- ¹⁹T. Kageyama, T. Miyamoto, M. Ohta, T. Matsuura, Y. Matsui, T. Furuhashi, and F. Koyama, *J. Appl. Phys.* **96**, 44 (2004).
- ²⁰Y.-H. Qu, D.-S. Jiang, D.-H. Wu, Z.-C. Niu, and Z. Sun, *Chin. Phys. Lett.* **22**, 2088 (2005).
- ²¹J. Thoma, B. Liang, Ch. Reyner, T. Ochalski, D. Williams, S. P. Hegarty, D. Huffaker, and G. Huyet, *Appl. Phys. Lett.* **102**, 013120 (2013).
- ²²O. Dier, S. Dachs, M. Grau, Ch. Lin, Ch. Lauer, and M.-Ch. Amann, *Appl. Phys. Lett.* **86**, 151120 (2005).
- ²³S. Mazzucato, R. J. Potter, A. Erol, N. Balkan, P. R. Chalker, T. B. Joyce, T. J. Bullough, X. Marie, H. Carrere, E. Bedel, G. Lacoste, A. Arnoult, and C. Fontaine, *Physica E (Amsterdam)* **17**, 242 (2003).
- ²⁴X. Liang, D. Jiang, B. Sun, L. Bian, Z. Pan, L. Li, and R. Wu, *J. Cryst. Growth* **243**, 261 (2002).
- ²⁵M. A. Pinault and E. Tournié, *Appl. Phys. Lett.* **78**, 1562 (2001).
- ²⁶Y. P. Varshni, *Physica (Utrecht)* **34**, 149 (1967).
- ²⁷M. Sun, P. J. Simmonds, R. B. Laghumavarapu, A. Lin, Ch. J. Reyner, H. S. Duan, B. Liang, and D. L. Huffaker, *Appl. Phys. Lett.* **102**, 023107 (2013).
- ²⁸L. Chen, V. G. Stoleru, and E. Towe, *IEEE J. Sel. Top. Quantum Electron.* **8**, 1045 (2002).